



Cite this: *Chem. Commun.*, 2014, 50, 13917

Received 14th August 2014,  
Accepted 10th September 2014

DOI: 10.1039/c4cc06385f

www.rsc.org/chemcomm

## Novel triarylamine-based polybenzoxazines with a donor–acceptor system for polymeric memory devices†

Lu-Chi Lin,‡ Hung-Ju Yen,‡ Chih-Jung Chen, Chia-Liang Tsai and Guey-Sheng Liou\*

**Novel polybenzoxazines consisting of electron-donating triphenylamine derivatives and electron-withdrawing 4,4'-diphenyl sulfone moieties were successfully prepared by the thermally induced ring-opening reaction of the corresponding PB precursors and utilized for memory devices.**

Polymeric memory materials have attracted increasing attention over the years since the first one was reported by Sliva *et al.*<sup>1</sup> in 1970, due to a growing demand for the establishment of next generation memory devices characterized by higher data storage density, longer data retention time, high speed, low power consumption, and low cost.<sup>2</sup> Polymeric memory materials store information in the form of a high (ON) and a low (OFF) current state in place of the amount of charges stored in a cell of silicon devices and have the advantages of a low-cost, solution processability, flexibility, and three-dimensional stacking capability for practical applications.<sup>3</sup> Hence, they are likely to be the next generation materials for memory devices. Triphenylamine (TPA) and its derivatives are well-known candidates for hole transport materials in organic optoelectronic devices due to the resulting stable radical cations and high hole-mobility.<sup>4</sup> Besides, the introduction of TPA units into the polymers could be expected to enhance the thermal stability as well as the glass transition temperature ( $T_g$ ) due to its high aromatic content. In recent years, there have been many research studies using TPA-based polymers as electro-active layers in the field of electrochromic<sup>5</sup> and memory applications.<sup>6</sup> In 2006, Kang *et al.* first demonstrated the electrical switching phenomenon of the TPA-based

polyimide **6F-TPA PI**,<sup>6a</sup> which behaved as a volatile dynamic random access memory (DRAM) characteristic. Recently, our group has systematically investigated donor, acceptor, and linkage effects on the memory behaviors,<sup>5g,6c-e</sup> and found that the polymers with the stronger electron donating/withdrawing units or non-planar linkage structure revealed longer retention time for their memory devices. Furthermore, TPA with electron-donating methoxy groups at the *para*-positions of phenyl units exhibited good electrochemical stability<sup>5b,6b</sup> and is expected to possess rewritable stability for memory devices.

It is well known that polybenzoxazine (PB) is a phenolic system with a wide range of interesting features and the capability to overcome several shortcomings of conventional novolac and resole type phenolic resins. These materials possess a near-zero volumetric change upon curing, low water absorption, excellent thermal resistance, good mechanical properties, dimensional stability, and low dielectric constant.<sup>7</sup> Thus, PBs are widely used in the areas of electrical insulation, electrical encapsulation, aeronautical and astronautical technologies. In this communication, we try to introduce donor–acceptor systems into PB precursors and the corresponding PBs, which were further fabricated into digital memory devices (Fig. 1). Novel PBs, **P(TPA-BPS)** and **P(TPPA-BPS)**, consisting of electron-donating TPA derivatives and electron-withdrawing diphenyl sulfone groups were prepared by the thermally induced ring-opening reaction of the corresponding PB precursors, **TPA-BPS** and **TPPA-BPS**, which were synthesized by the reaction of paraformaldehyde, TPA-based diamines [4,4'-diamino-4''-methoxytriphenylamine (**1**)<sup>5b</sup> and *N,N*-bis(4-aminophenyl)-*N,N'*-di(4-methoxyphenyl)-1,4-phenylenediamine (**2**)<sup>5c</sup>], and commercially available 4,4'-sulfonyldiphenol (BPS). The detailed synthetic procedure and basic properties are described in the ESI.† In order to investigate the acceptor effect on memory behaviors, PB precursors derived from bisphenol A (BPA)<sup>8</sup> are also utilized and discussed for comparison.

UV-vis absorption spectra of PBs are depicted in Fig. S3 (ESI†), and the onset wavelength of optical absorption was utilized to obtain the optical energy band gap ( $E_g$ ) of the PBs. The electrochemical properties of the PB precursors and PBs were investigated

Functional Polymeric Materials Laboratory, Institute of Polymer Science and Engineering, National Taiwan University, 1 Roosevelt Road, 4th Sec., Taipei 10617, Taiwan. E-mail: gsliau@ntu.edu.tw; Fax: +886-2-33665237; Tel: +886-2-33665315

† Electronic supplementary information (ESI) available: Experimental section. Results and discussion. Figure: <sup>1</sup>H NMR spectra, DSC, TGA, TMA, DMA, CV, UV-vis diagram of polymers. Scheme: synthesis of PB precursors; thermal ring opening polymerization mechanism of benzoxazines; increased intramolecular CT ways of PBs containing BPS. Table: inherent viscosity, molecular weight, and thermal properties. See DOI: 10.1039/c4cc06385f

‡ Authors L. C. Lin and H. J. Yen contributed equally to this work.

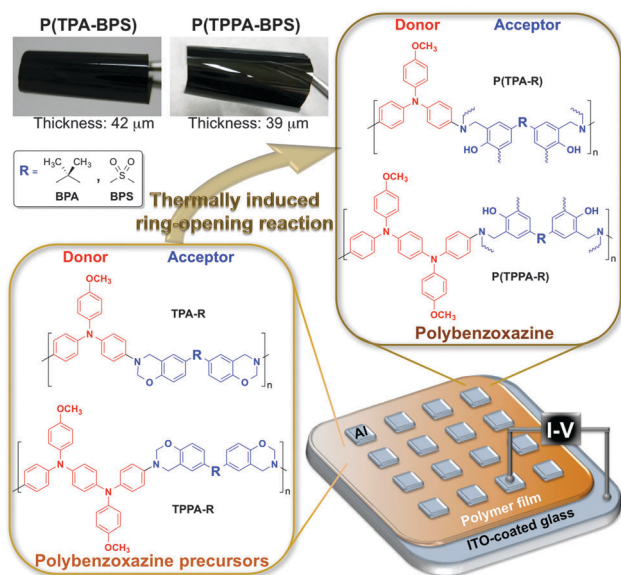


Fig. 1 Chemical structures of TPA-based resulting polymers and schematic diagram of the memory device consisting of a polymer thin film sandwiched between an ITO bottom electrode and an Al top electrode.

using cyclic voltammetry (CV) using a 0.1 M tetrabutylammonium perchlorate (TBAP) as the supporting electrolyte under a nitrogen atmosphere. The typical CV diagrams of PB precursors and PBs are depicted in Fig. S4 and S5 (ESI<sup>†</sup>), respectively. In solution-type CV, TPA-based and TPPA-based PB precursors reveal reversible oxidation redox couples with  $E_{1/2(\text{ox}1)}$  at around 0.50 V and 0.40 V, respectively. The film-type CV showed similar curves to that of solution-type CV. After the thermally induced ring-opening reaction, **P(TPA-BPS)** and **P(TPPA-BPS)** exhibited  $E_{1/2(\text{ox}1)}$  at 0.91 V and 0.69 V, respectively. The redox potentials of the polymers and their respective HOMO and LUMO (*versus vacuum*) were calculated and are summarized in Table 1.

The memory behaviors of PB precursors and PBs were depicted by the current–voltage ( $I$ – $V$ ) curves on an ITO/polymer/Al sandwich device as shown in Fig. 2, and the repeating cycle tests are also depicted in Fig. S6 (ESI<sup>†</sup>). Within the memory device, polymer films were used as an active layer with Al and ITO as the top and bottom electrodes, respectively. Polymer film thickness was

Table 1 Redox potentials and energy levels of PB precursors and PBs

Polymer	Oxidation potential (V) ( <i>vs.</i> Ag/AgCl)		UV-vis absorption (nm)		Energy levels (eV)		
	$E_{\text{ox,onset}}$	$E_{\text{ox},1}^{1/2}$	$\lambda_{\text{max}}$	$\lambda_{\text{onset}}$	$E_{\text{g}}^a$	HOMO <sup>b</sup>	LUMO
<b>TPA-BPA</b>	0.42	0.50	310	484	2.56	−4.75	−2.19
<b>TPA-BPS</b>	0.46	0.55	307	508	2.44	−4.80	−2.36
<b>TPPA-BPA</b>	0.29	0.40	317	512	2.42	−4.65	−2.23
<b>TPPA-BPS</b>	0.29	0.44	315	513	2.42	−4.69	−2.27
<b>P(TPA-BPS)</b>	0.62	0.91	294	518	2.39	−5.25	−2.86
<b>P(TPPA-BPS)</b>	0.45	0.69	305	523	2.37	−5.03	−2.66

<sup>a</sup> The data were calculated from polymer films by the equation:  $E_{\text{g}} = 1240/\lambda_{\text{onset}}$  (energy gap between HOMO and LUMO). <sup>b</sup> The HOMO energy levels were calculated from cyclic voltammetry and were referenced to ferrocene (4.8 eV;  $E_{1/2} = 0.55$  V in  $\text{CH}_2\text{Cl}_2$ , 0.46 V in  $\text{CH}_3\text{CN}$ ).

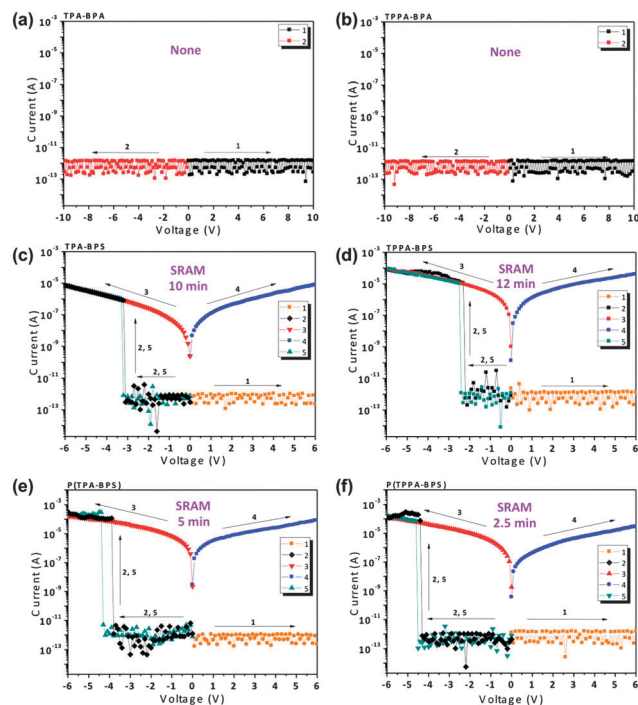


Fig. 2 Current–voltage ( $I$ – $V$ ) characteristics of the ITO/polymer (50 ± 3 nm)/Al memory device. (a) **TPA-BPA**, (b) **TPPA-BPA**, (c) **TPA-BPS**, (d) **TPPA-BPS**, (e) **P(TPA-BPS)**, and (f) **P(TPPA-BPS)**.

optimized around 50 nm and was used for all devices. Fig. 2a and b showed the  $I$ – $V$  results of BPA-derived PB precursors, **TPA-BPA** and **TPPA-BPA**, respectively. Both the devices kept at a low-conductivity (OFF) state during both positive and negative scans, indicating an insulator characteristic and can be ascribed to a weak donor–acceptor capability within the polymer chains. In contrast, Fig. 2c and d depicted the  $I$ – $V$  results of the BPS containing PB precursors, **TPA-BPS** and **TPPA-BPS**, respectively. During the first positive sweep from 0 V to 6 V, the devices stayed in the low-conductivity (OFF) state with a current range of  $10^{-12}$  to  $10^{-13}$  A, implying that the positive applied voltage cannot switch both of the memory devices on. In contrast, during the second sweep from 0 V to −6 V, the current maintained around  $10^{-12}$ – $10^{-13}$  A followed by a rapid increase to  $10^{-5}$  A and  $10^{-4}$  A (high-conductivity state) corresponding to the threshold voltage of −3.1 V (**TPA-BPS**) and −2.2 V (**TPPA-BPS**), respectively, indicating the transition from the OFF state to a high-conductivity (ON) state with an ON/OFF current ratio of  $10^6$ – $10^7$ . For memory device, this OFF-to-ON transition can be defined as a “writing” process. Two devices remained in the ON state during the subsequent negative scans (line 3) and then positive scans (line 4). Therefore, the memory devices based on **TPA-BPS** and **TPPA-BPS** cannot be reset to the initial OFF state by applying a reverse electric field exhibiting non-erasable behavior. Interestingly, the ON state could also remain once the memory devices have been switched to the ON state, even after turn off power for an extended period of time. The fifth sweep of the devices was conducted after turning off the power for about 10 min (**TPA-BPS**) and 12 min (**TPPA-BPS**), respectively; it was found

that the ON state could be relaxed to the original OFF state without an erasing process. During the fifth sweep, the device could be switched to the ON state again at the threshold voltage of  $-3.2$  V (TPA-BPS) and  $-2.4$  V (TPPA-BPS), respectively. Thus, these two devices with long retention time behave as a SRAM characteristic, and TPPA-BPS with stronger electron-donating capability showed longer retention time as opposed to TPA-BPS.<sup>6c</sup>

Furthermore, we investigated the memory characteristics of BPS-based PBs, P(TPA-BPS) and P(TPPA-BPS), which were prepared by the thermally induced ring-opening reaction. In the case of P(TPA-BPS) (Fig. 2e), the memory device can be switched to the ON state at the switch-on voltage of  $-3.8$  V (line 2) and remains at the ON state during the subsequent negative scan (line 3) and then positive scan (line 4). The ON state could be kept after turn off the power up to 5 min, indicating a volatile SRAM memory property. The shorter retention time of P(TPA-BPS) than the corresponding precursor TPA-BPS could be attributed to the formation of intramolecular hydrogen bonding and more route for back charge transfer (CT) in the network structures of PBs (Scheme S3, ESI<sup>†</sup>). The electrochromism of BPA-based PBs has been investigated by us very recently, and found that the formation of intramolecular hydrogen bonding between the active nitrogen sites of TPA-based diamine moieties and hydroxyl groups of the BPA units in the network structures of PBs, which would result in a lowered electron-donating ability of the electro-active nitrogen sites of the triarylamine diamine moieties in the cured PBs.<sup>8</sup> In addition, Chen and Ueda have also demonstrated the effect of flexible ether linkages between donor and acceptor and found that the fewer the ether linkages introduced into polymer chain (more direct intramolecular CT), the shorter the retention time memory device performed.<sup>9</sup> The above investigations further confirmed our finding that the PBs exhibit shorter retention time as opposed to the corresponding PB precursors. P(TPPA-BPS) (Fig. 2f) showed similar SRAM memory behavior to P(TPA-BPS) (Fig. 2e) with the switch-on voltage of  $-4.3$ , but the ON state could only be kept for 2.5 min after turning off the power even when a stronger electron-donating group (tetraphenyl-*p*-phenylenediamine) was introduced.

In order to get more insight into the memory behaviors of these PB precursors and PBs, a molecular simulation of the basic unit was carried out using DFT/B3LYP/6-31G(d) and the Gaussian 09 program as shown in Fig. 3. The HOMO and LUMO energy levels calculated by molecular simulation were in agreement with the tendency of experimental values, and the charge density isosurfaces of the basic unit were summarized. According to a previous literature,<sup>6a</sup> when the applied electric field reaches the switching-on voltage, some electrons at the HOMO accumulate energy and transit to the LUMO, forming a charge transfer complex (ON state) by different ways. For all PB precursors and the corresponding PBs containing BPS, the HOMO is located mainly at the electron-donating TPA moieties, while LUMO is distributed around the electron-withdrawing BPS moieties. Using TPA-BPS as an example, when the applied electric field reaches the switching-on voltage, some electrons at HOMO accumulate energy and transit to LUMO7 due to the

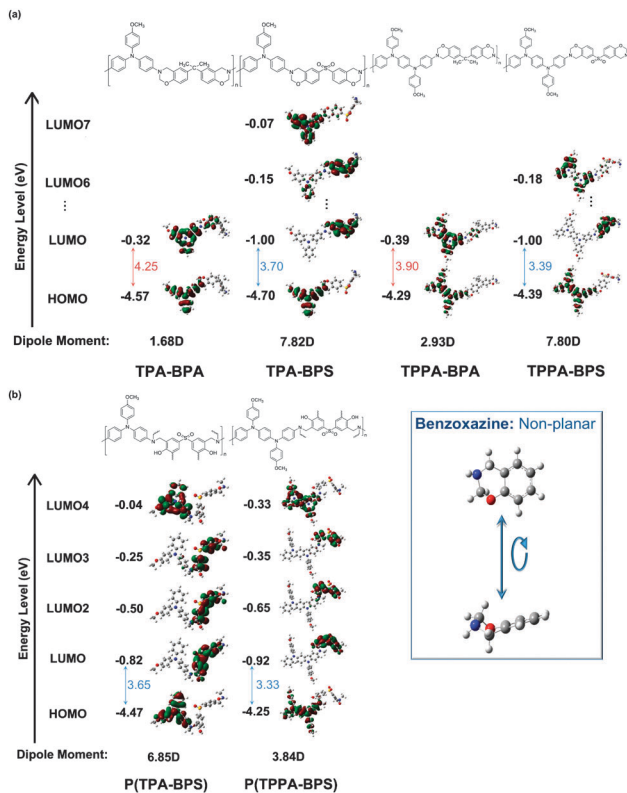


Fig. 3 Calculated molecular orbitals and corresponding energy levels of the basic units for (a) PB precursors and (b) PBs.

highest possibility/overlapping of electron distribution between HOMO and LUMO.7 Nevertheless, electrons at HOMO may also be excited to the other intermediate LUMOs with a lower energy barrier belonging to the acceptor units. Thus, CT occurs through several courses to form the conductive CT complexes, including indirectly drop from LUMO7 through intermediate LUMOs to LUMO, from the intermediate LUMOs to LUMO, or directly be excited from HOMO to LUMO. When the intra- or intermolecular CT occurs due to the applied electric field, the generated holes can delocalize to the TPA moieties forming an open channel in the HOMO for the charge carriers (holes) to migrate through. Therefore, the current increases rapidly and the memory device can be switched to the high conductivity state (ON state). In addition, our group has also investigated the linkage effect on the memory behavior and found that the polymer with more non-planar linkage revealed longer retention time (Fig. 3a).<sup>6d,e</sup> Therefore, both BPS-based PB precursors, TPA-BPS and TPPA-BPS, exhibited SRAM behavior due to the incorporation of non-planar benzoxazine groups and high dipole moments, which can further stabilize the CT complex. Moreover, the higher dipole moment of P(TPA-BPS) leads to a longer retention time than P(TPPA-BPS) (Fig. 3b).

In summary, new polybenzoxazines containing electron-donating triarylamine and electron-accepting diphenyl sulfone groups have been successfully prepared by the thermally induced reaction of the corresponding precursors and fabricated for memory device application. All the BPS-based polymers exhibited

SRAM properties with retention time ranging from 2.5 to 12 min. To the best of our knowledge, this is the first time that the memory characteristics of PB precursors and PBs with triarylamine moieties have been investigated.

## Notes and references

- 1 P. O. Sliva, G. Dir and C. Griffiths, *J. Non-Cryst. Solids*, 1970, **2**, 316.
- 2 (a) H. Gruber, *Resour. Policy*, 2000, **29**, 725; (b) S. Moller, C. Perlov, W. Jackson, C. Taussig and S. R. Forrest, *Nature*, 2003, **426**, 166.
- 3 A. Stikeman, *Technol. Rev.*, 2002, **105**, 31.
- 4 (a) Y. Shirota, *J. Mater. Chem.*, 2005, **15**, 75; (b) K. Y. Chiu, T. H. Su, C. W. Huang, G. S. Liou and S. H. Cheng, *J. Electroanal. Chem.*, 2005, **578**, 283.
- 5 (a) S. H. Cheng, S. H. Hsiao, T. H. Su and G. S. Liou, *Macromolecules*, 2005, **38**, 307; (b) C. W. Chang, G. S. Liou and S. H. Hsiao, *J. Mater. Chem.*, 2007, **17**, 1007; (c) H. J. Yen and G. S. Liou, *Chem. Mater.*, 2009, **21**, 4062; (d) H. J. Yen, H. Y. Lin and G. S. Liou, *Chem. Mater.*, 2011, **23**, 1874; (e) L. T. Huang, H. J. Yen and G. S. Liou, *Macromolecules*, 2011, **44**, 9595; (f) H. J. Yen and G. S. Liou, *Polym. Chem.*, 2012, **3**, 255; (g) H. J. Yen, C. J. Chen and G. S. Liou, *Adv. Funct. Mater.*, 2013, **23**, 5307; (h) Y. W. Chuang, H. J. Yen and G. S. Liou, *Chem. Commun.*, 2013, **49**, 9812.
- 6 (a) Q. D. Ling, F. C. Chang, Y. Song, C. X. Zhu, D. J. Liaw, D. S. H. Chan, E. T. Kang and K. G. Neoh, *J. Am. Chem. Soc.*, 2006, **128**, 8732; (b) T. J. Lee, Y. G. Ko, H. J. Yen, K. Kim, D. M. Kim, W. Kwon, S. G. Hahm, G. S. Liou and M. Ree, *Polym. Chem.*, 2012, **3**, 1276; (c) C. J. Chen, H. J. Yen, Y. C. Hu and G. S. Liou, *J. Mater. Chem. C*, 2013, **1**, 76232; (d) C. J. Chen, Y. C. Hu and G. S. Liou, *Chem. Commun.*, 2013, **49**, 2536; (e) C. J. Chen, Y. C. Hu and G. S. Liou, *Polym. Chem.*, 2013, **4**, 4162; (f) L. Shi, H. Ye, W. Liu, G. Tian, S. Qi and D. Wu, *J. Mater. Chem. C*, 2013, **1**, 7387; (g) C. J. Chen, Y. C. Hu and G. S. Liou, *Chem. Commun.*, 2013, **49**, 2804; (h) C. J. Chen, J. H. Wu and G. S. Liou, *Chem. Commun.*, 2014, **50**, 4335.
- 7 (a) H. Ishida, in *Handbook of Benzoxazine Resins*, ed. H. Ishida and T. Agag, Elsevier, Amsterdam, 2011, pp. 3–81; (b) X. Ning and H. Ishida, *J. Polym. Sci., Part A: Polym. Chem.*, 1994, **32**, 1121; (c) Y. L. Hong and H. Ishida, *Macromolecules*, 1997, **30**, 1099; (d) T. Takeichi, T. Kano and T. Agag, *Polymer*, 2005, **46**, 12172; (e) N. N. Gosh, B. Kiskan and Y. Yagci, *Prog. Polym. Sci.*, 2007, **32**, 1344; (f) C. H. Lin, S. L. Chang, T. Y. Shen, Y. S. Shih, H. T. Lin and C. F. Wang, *Polym. Chem.*, 2012, **3**, 935; (g) C. H. Lin, Y. S. Shih, M. W. Wang, C. Y. Tseng, T. Y. Juang and C. F. Wang, *RSC Adv.*, 2014, **4**, 8692.
- 8 L. C. Lin, H. J. Yen, Y. R. Kung, C. M. Leu, T. M. Lee and G. S. Liou, *J. Mater. Chem. C*, 2014, **2**, 7796.
- 9 T. Kuorosawa, C. C. Chueh, C. L. Liu, T. Higashihara, M. Ueda and W. C. Chen, *Macromolecules*, 2010, **43**, 1236.